Journal of Physics: Conference Series **248** (2010) 012038 doi:10.1088/1742-6596/248/1/012038

Experimental and theoretical investigation on high-Tc superconducting intrinsic Josephson junctions

Alexander Grib[1,2], Yury Shukrinov[3], Frank Schmidl[1], Paul Seidel[1]

[1] Institut für Festkörperphysik, Friedrich-Schiller-Universität Jena, D-07743 Jena, Germany
[2] Physics Department, V. N. Karazin Kharkiv National University, 61077 Kharkiv, Ukraine
[3] Joint Institute for Nuclear Research, BLTP, Dubna, 141980, Russia

E-mail: "Paul Seidel" <Paul.Seidel@uni-jena.de>

Abstract. Within the last years many groups have realized and investigated different types of intrinsic Josephson junction (IJJ) arrays out of high-temperature superconducting single crystals or thin films. We tried to improve the synchronization between the junctions by external shunts. Mesa structures as well as microbridges on vicinal cut substrates showed multi-branch behaviour in their IV characteristics and random switching between branches. Theoretical modelling was done investigating phase dynamics and stability numerically as well as analytically. Branch structure in current voltage characteristics of IJJ is studied in the framework of different models, particularly, in capacitevely coupled Josephson junctions (CCJJ) model and CCJJ model with diffusion current. Results of modelling of return current in IV characteristics for stacks with different number of IJJ are presented. We discussed the possible mechanisms of synchronization and the ranges of stability. Conclusions with respect to application of such arrays such as radiation sources were given.

1. Introduction

Since the discovery of the intrinsic Josephson effects by Kleiner et al. [1] there are a lot of works concerning the physics of the intrinsic junctions, e.g. [2-13]. Thus we will restrict ourself here to facts which are relevant for application. The intrinsic Josephson effects in the cuprates where the superconducting CuO_2 - planes are coupled via non-superconducting barrier layers within the unit cell of the materials can be used to produce series junction arrays. The number of junctions depends on the thickness of the high-Tc material between the electrodes. Optimization of technology and a complex control of the preparation process allows to reduce the number of junctions to a few or even a single one. There are different technologies using mesa geometry of vertical stacks, stacks grown at steps in the substrate, focussed ion beam cutted single crystal or film structures and planar "horizontal stacks" grown on vicinal cutted substrates. Additional doping or external shunting of the intrinsic arrays can be used to adjust the junction parameters or to enhance the synchronization of the junctions within the array. In this way the weak coupling is realized in a periodic stack of Josephson junctions with atomic dimensions along the crystallographic c-axis. These intrinsic Josephson junctions can be described by the Josephson or more general weak link physics but the small dimensions as well as the series connection of

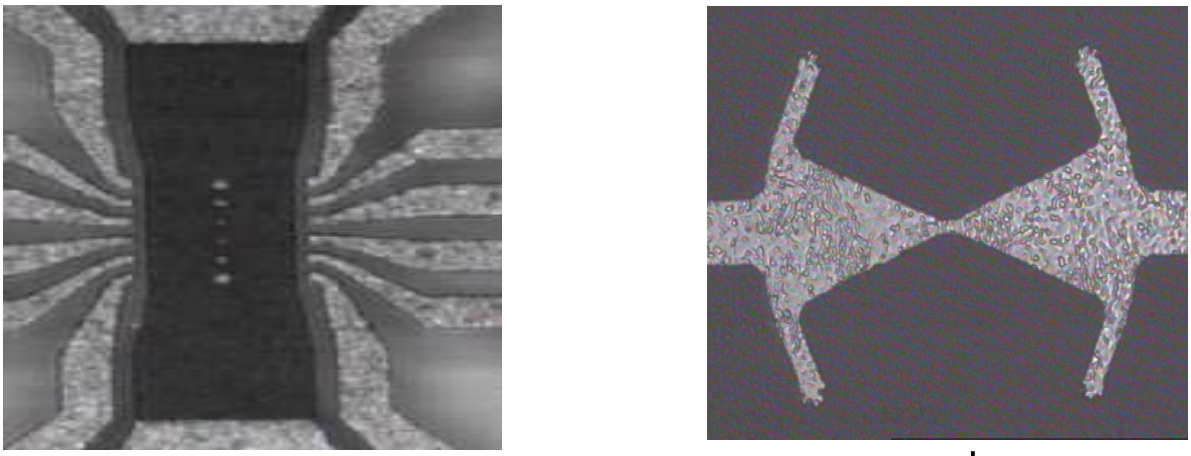

Figure 1. Two types of thin film intrinsic Josephson junctions. (a) 6 Tl-2212 mesas with areas from 2x2 μm^2 to 5x5 μm^2 in the center of the substrate before they were covered by a gold contact which is cut by ion etching to get separate contacts for 4-point measurement; (b) the microbridge on vicinal cut substrate with a 2x2 μm^2 *planar* stack imbedded in an antenna structure (Tl-2212 on 20 degrees vicinal cut $LaAlO_3$)

many junctions gives rise to some special behaviour and parameters. Modeling of the junctions has to take into account these special properties. Some examples will be given here.

2. Preparation of junctions

While the first investigations on the intrinsic junctions used single crystals or etched parts out of them, different thin film technologies have been developed meanwhile, too. Thin film structures used a mesa-type geometry where the high-Tc film is patterned with lateral dimensions in the μm-range, e.g. [14, 15] and references therein. The problem of metal electrodes to the mesas was solved even for a four-point-measurement which requires two separated contacts on top of each mesa like in Fig. 1a, see Seidel et al. [16] . A very interesting technology of preparation of quite homogeneous and well-defined junction arrays was proposed by Kim et al. [17] for single crystal whiskers and later adapted to single crystal pieces mounted on substrates [6]. Focused ion beams were used to etch the small well-defined stack of junctions out of the material from two sides in a way that the remaining high-Tc materials act as electrodes to the stack. By this "double-sided fabrication method" or "flip-chip technique" the quality and homogeneity of the intrinsic junction arrays was dramatically improved. On the other side technologies were developed to realize a very small junction number down to the single junction limit, see e.g. [4], [18], and [19]. Koval et al. [20] showed that T_C, I_C and R_n of intrinsic Bi-2212 Josephson junctions can be tuned in a large range by current injection. This carrier injection effect is reversible and persistent. An alternative way to realize a thin film intrinsic stacked junction array uses substrates with a surface not parallel to the CuO_2-planes [21]. On such vicinal cutted substrates the film growths with CuO_2-planes tilted with respect to the surface. Patterning of a microbridge results in a nearly horizontal stack of junctions and the length of the microbridge corresponds to the number of junctions in series, see Fig. 1b. Intrinsic Josephson behavior of the microbridges was observed for misorientation angles equal or larger than 15 degrees [22]. This kind of arrays offers new possibilities for synchronization [23].

3. Experiments and results

The superconducting CuO_2 -planes in IJJ are separated by coupling layers of some tenth of a nanometer. This leads to many differences compared to artificial prepared planar barrier junctions with quite compact superconducting electrodes and much thicker single barrier layers. The other main difference is that intrinsic junctions are naturally series arrays instead of single junctions. Thus the observed IV-characteristic is a sum of single junctions characteristics leading to many branches up to high voltages, see Fig. 2a. For very high voltages the heat dissipation leads to non-equilibrium effects and negative differential resistance parts in the IV. While the number of junctions in the intrinsic arrays is quite easy to control by thickness of the stack of superconducting unit cells their homogeneity is still a problem. Thus there is a quite large spread in single junction parameters. If the spread can be reduced the internal synchronization of the junctions improves the dynamic of these arrays. Additional shunting or resonance environment can further improve the synchronization leading to a collective many-junction behavior [24-26]. This is of relevance e.g. for radiation sources realized by intrinsic arrays. The lateral dimensions of intrinsic Josephson junctions play a crucial role, too. Perpendicular to the atomic arrays there is flux-flow of Josephson vortices corresponding to these dimensions. This results in plasma waves and additional dynamic effects. On one side such effects can be applied for radiation sources [10, 11] on the other side they lead to a complex behavior and additional noise contributions, see e.g. [8] , [10], [27], [28] and references therein.

4. Synchronization

One of the most important applications of the intrinsic Josephson effect is the construction of sub-microwave sources of coherent radiation. The common synchronizing ac current in all junctions is the condition of strong synchronization. Radiation of synchronizing junctions itself can produce this ac current if there is a feedback in the system. The existence of the current resonant mode in the system provides both the strong ac current produced by radiation of junctions and a strong feedback. Thus, an application of a superconducting resonator is a solution to obtain synchronization of Josephson junctions. It was shown in [24] that the synchronizing ac current is largest in serial arrays of junctions. Intrinsic Josephson junctions satisfy the requested conditions and small spread of critical currents and normal resistances can be in principle achieved. In the present paper we present results of numerical and analytical investigations [23, 25, 28] and experiments [23] for stacks of junctions in a resonator. In our 'lumped' analysis the Josephson junction is always the parallel connection of the source of Josephson current I_c, the resistance R_n and the capacitance C (this is a so-called extended resistively shunted model of a junction). The resonator is always modeled as a parallel connection of some capacitance C_{res} and an inductance L_{res}, so the resonance frequency is $\frac{1}{\sqrt{L_{res}C_{res}}}$. At first, we present results for synchronization of stacks of 'classical' junctions, i.e. junctions which are separated by large distances of superconductor which have the constant order parameter, and then we discuss the specific features of synchronization of intrinsic junctions. The system of differential equations for phase dynamic of N junctions with different loads can be represented schematically as follows:

$$\left(1-(-1)^k\,\delta\right)\left(\beta_C\ddot{\varphi}_k\left(\tau\right)+\dot{\varphi}_k+sin\left(\varphi_k\right)\right)=i_b-\tilde{i_k}$$
$$\sum\dot{\varphi}_k=D\left(\tilde{i_k}\right), \qquad (1)$$

where k is the number of the junction, δ is spread of critical currents, $\tilde{i_k}$ is the ac current flowing in the junctions due to a feedback, φ_k, $\dot{\varphi}_k$ and $\ddot{\varphi}_k$ are the phase difference across k-th junction and its first and second derivative with respect to the dimensionless time $\tau=\frac{2\pi R_n I_c t}{\Phi_0}$ with Φ_0 as the quantum of magnetic flux, i_b is the dc bias current (all small letters here and further denote

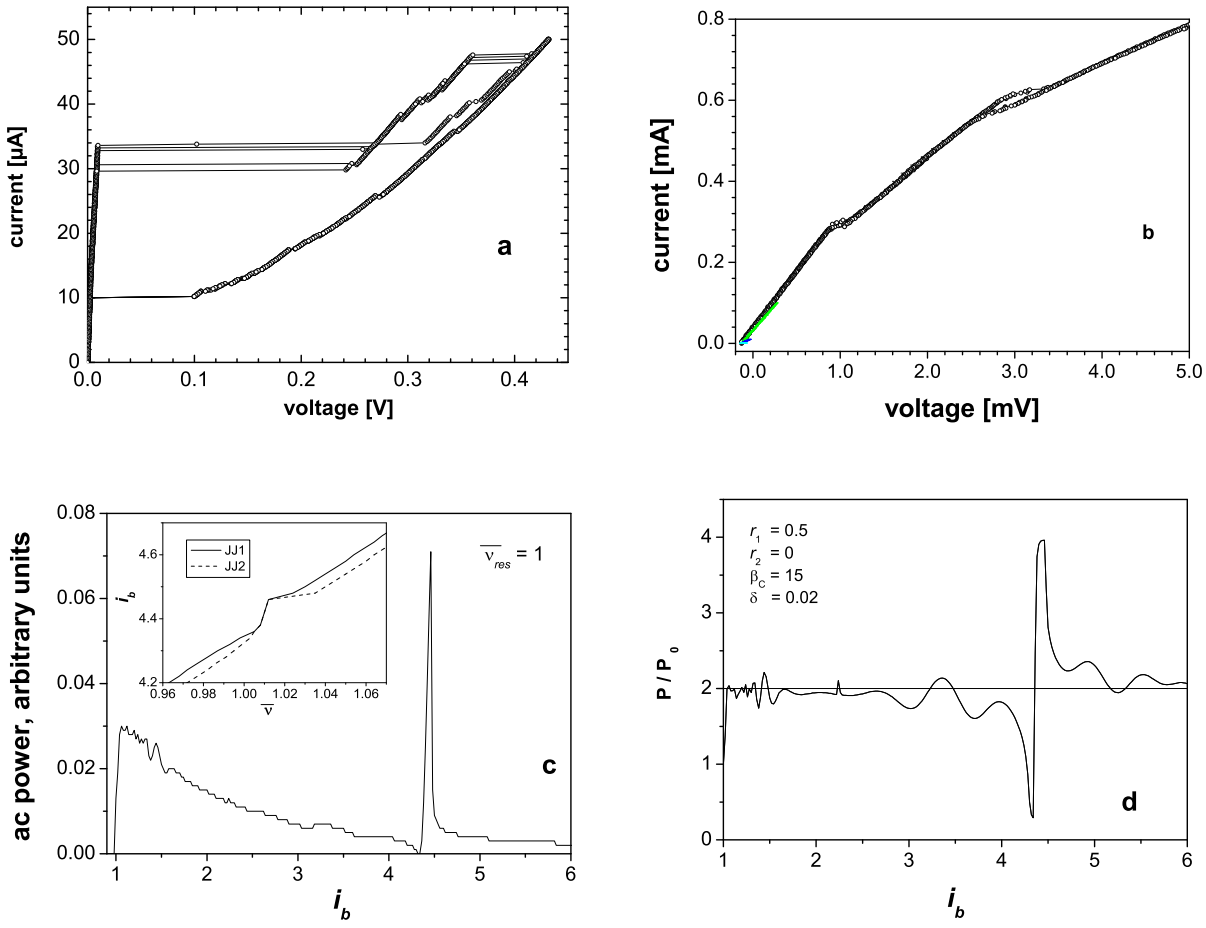

Figure 2. IV-characteristics measured with the use of the current-biased scheme for the microbridge in the resonator without the shunt (a) and with the gold shunted cover (b); the calculated dependence of emitted power plotted as a function of the bias current for the shunted chain of two junctions in the resonator (c) and the emitted power normalized with respect to the power of the single junction (d). In the inset in (c) the IV-characteristics of both junctions are shown.

normalized units, see Ref.[24], impedances are normalized with respect to R_n and voltages across junctions measured in units of I_cR_n are $\dot{\varphi_k}$), β_C is the McCumber parameter and $D\left(\tilde{i_k}\right)$ is the differential equation which determines the ac current in the load which is different for various types of the load. With the use of Eqs. (1) we modeled phase dynamic of a stack of Josephson junctions connected on ends with several types of loads, namely the resistive matched shunt, the sequential LC-resonant contour and a resonant transmission line with open ends. We found that the LC-contour and a resonant transmission line provide the maximal tolerant spread of critical currents (about 15 %), whereas for the matched load this value is only about 7 % [23, 25]. The parameters of transmission line appeared to be hard to regulate and, therefore, the most optimal choice for the synchronization system is the superconducting resonator. We note that some reasonable resistive losses in the resonator decrease the maximal tolerant spread to 10-12 %.

The optimal parameters provide strong synchronization for the stack of Josephson junctions

with the resonator up to 15% is $\beta_C = 0.8 - 1.3$, $\beta_{Cres} = 0.4 - 0.6$ and $\beta_{Lres} = 3 - 5$ (here $\beta_{Cres} = \frac{2\pi I_c R_n^2 C_{res}}{\Phi_0}$ and $\beta_{Lres} = \frac{2\pi I_c L_{res}}{\Phi_0}$ are the reduced capacitance and the reduced inductance of the contour, correspondingly). These values are far from those of intrinsic junctions ($\beta_C = 10 - 30$). Therefore, we tried to decrease the McCumber parameter by the external shunting. We covered the chain of intrinsic junctions by the resistive shunt to decrease the McCumber parameter. For the experiments we used $Tl_2Ba_2CaCu_2O_8$ films grown epitaxially on 20 degrees misaligned $LaAlO_3$ in a two-step process [23]. The system was implemented into a resonant structure with a resonant frequency of about 500 GHz, see Fig. 1b. Microbridges were covered by a 10 nm shunting gold layer. The thickness of the shunt in first measurements is about 30 nm that provided a resistance of the shunt per junction of about 1 Ohm. Each of the microbridges was consisted of about 400 junctions. In Fig. 2a we show IV- characteristics for microbridges which gold layer is etched away (i.e. the microbridge was not shunted). This IV-characteristic shows the multibranch behaviour. The effect of the multibranch behaviour is almost absent in the IV-characteristic of the shunted microbridge (Fig. 2b). We modeled the emitted power of the shunted microbridge in the resonator for two junctions with the small spread of critical currents and found that the line of the coherent generation can be very narrow (Fig. 2c). The normalized ac power P/P_0 of radiation showed in-phase synchronization of junctions (Fig. 2d, values of P/P_0 are equal to 0, 2 and 4 if there is anti-phase synchronization, no synchronization and in-phase synchronization, correspondingly). However, there are optimal parameters for the in-phase synchronization. We calculated the optimal parameters of the system for the shunting microbridges. The maximal tolerant spread of critical currents in this case is equal to about 26 % [24]. It is possible for junctions with the value of the McCumber parameter of about 15 when the resistances of the shunt and the interface between the shunt and the junctions are equal to 0.5 and 0.01 parts of the resistance of the junction and the resonant frequency is about 1/3 of the characteristic frequency of the junction. In our experiment, the resonant frequency and the resistance of the interface is close to this optimal frequency, though the resistance of the shunt was too low. Despite of some disparity of parameters, the measured IV-characteristic of the microbridge (Fig.2b) shows the absence of branches and the break which is characteristic for the behaviour of IV-characteristics in the resonator. The absence of branches shows that the junctions can be synchronized, though the check of this fact requires the straightforward measurements of the emitted radiation. In our calculations, we found that the effect of the multibranch behaviour impedes synchronization and one should avoid to apply the resonant frequency in the region of the multibranch behaviour. The narrow-band sychronization of two junctions is calculated in Figs. 2c, d for the region of the IV-characteristic above the hysteretic region. There is a way to use the successive set of capacitances of junctions as a capacitance of the resonator. In this case junctions with the spread of critical currents of about 10% are strongly synchronized in the hysteretic region [28]. We would like to note that the frequency spectrum of radiation in the hysteretic region contains many harmonics, and the same principle as used in Ref.[28] gives the best results in the non-hysteretic region, i.e. above the characteristic frequencies of the junctions. In this case the line of the in-phase generation has only one main harmonic.

5. Return current

The temperature dependence of the return current of single junction is determined by the temperature dependence of the critical current and the McCumber parameter β_C. For the coupled system of Josephson junctions it is additionally determined by the number of junctions in the stack, by the coupling between junctions and boundary conditions. The temperature dependence of β_C in its turn depends on the temperature dependence of the critical current $I_C(T)$, junction resistance $R_J(T)$ and capacitance $C_J(T)$. In present paper we assume that the capacitance of the junctions is the temperature independent geometrical capacitance

$C_J = \varepsilon_r \varepsilon_0 S/D$, where S is the area of the junctions, ε_r is dielectric constant, ε_0 is electric constant, and D is the thickness of the insulating layer. In the capacitively coupled Josephson junctions model with diffusion current (CCJJ+DC model),[29, 30] the stack with N intrinsic Josephson junctions is described by a system of dynamical equations for the gauge-invariant phase differences $\varphi_l(t) = \theta_{l+1}(t) - \theta_l(t) - \frac{2e}{\hbar}\int_l^{l+1} dz A_z(z,t)$ between superconducting layers (S-layers). Here θ_l is the phase of the order parameter in S-layer l, A_z is the vector potential in the barrier. To investigate the temperature dependence of different characteristics of IJJ, and to compare results at different temperatures, it's suitable to normalize all values to the parameters at $T = 0$, because I_c, ω_p, R_J, and β depend on temperature. In this case the system of equations has a form

$$\begin{aligned} \frac{d}{dt}V_l &= I - J_c \sin\varphi_l - \tilde{\beta}\frac{d\varphi_l}{dt} \\ \frac{d}{dt}\varphi_l &= V_l - \alpha(V_{l+1} + V_{l-1} - 2V_l), \end{aligned} \tag{2}$$

where time is $\tau * \omega_{p0}$ ($\omega_{p0}^2 = 2eI_{c0}/\hbar C$), current is normalized to I_{c0}, the voltage - to the value $V_0 = \hbar\omega_{p0}/2e$, and $\tilde{\beta} = 1/(\omega_{p0}R_j C) = \beta\sqrt{J_c}$. I.e., the behavior of system is determined by parameters α, J_c and $\tilde{\beta}$. Compared to the single Josephson junction, the system of the coupled Josephson junctions has a multiple branch structure and the definition of the return current is more general now: the system can return to this state from any branch and the value of the return current depends on from which one the system has returned to the zero voltage state. In our simulation we calculate the return current from the first branch. We fix the temperature and determine the corresponding value of the dissipation parameter β. Then, at these values of β, we solve numerically [31, 32] the system of dynamical equations (2). It allow us to get the CVC of the first branch and find the value of the return current. Then we repeat the procedure for another value of temperature.

We compare the results of numerical simulation of the temperature dependence of the return current with the dependence of the Zappe model [33, 34] calculated by formula

$$I_r(T) = I_c(T)\frac{-(\pi-2) + \sqrt{(\pi-2)^2 + 8\beta_c}}{2\beta_c} \tag{3}$$

with the same fitted dissipation parameter β. Zappe model with Heine resistivity [34] can not be used to explain strong temperature dependence of the return current in $Bi_2Sr_2CaCu_2O_x$ intrinsic Josephson junctions because it does not include the coupling between junctions in the stack. The influence of the coupling between junctions on the return current can be investigated directly by numerical methods.

Here we present two results on simulation of the temperature dependence of the return current. One is based on the fitting of the temperature dependence tunnel resistivity of the Josephson junction. For critical current is assumed the Ambegaokar-Baratoff dependence [35]. Another one used fitting of the experimental results on of critical current and McCumber parameter. In the simple parallel resistance model [36] a single junction resistivity $\rho_J(T)$ at subgap voltage region is given by $\rho_J^{-1}(T) = \rho_{sg}^{-1} + \rho_C^{-1}(T)$, where ρ_{sg} is the temperature independent tunnel resistivity of the junction, and $\rho_C(T) = a\exp(b/T) + cT + d$ is the empirical Heine formula of the c-axis resistivity [34] with a, b, c, d as fitting parameters. At low temperature c-axis resistance freezes out, and the junction resistance is dominated by the temperature independent term ρ_{sg}.

Estimating the tunnel resistivity by $\rho_{sg} = \Delta(0)S/eDI_c(0)$, the energy gap Δ from the expression $2\Delta(0)/kT_c = 6$ and using the equation for $\rho_C(T)$, we can find the temperature

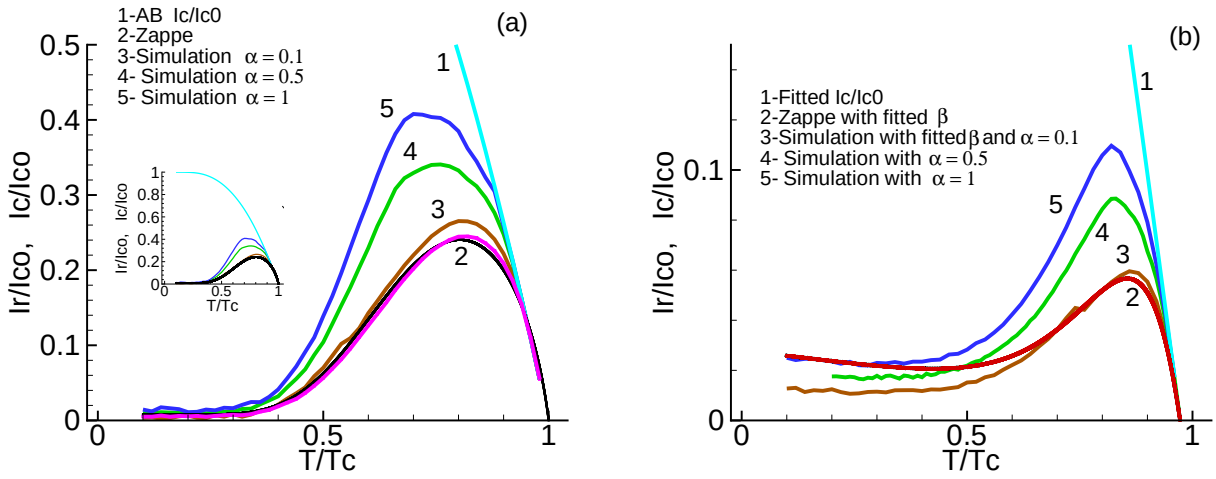

Figure 3. (Color online) (a) - the simulated temperature dependence of the return current I_r at different values of the coupling parameter α together with the Ambegaokar-Baratoff dependence of the critical current I_c. (b) - the simulated temperature dependence of the return current I_r at different values of the coupling parameter α with fitted critical current I_c.

dependence of the junction resistance $R_J = \frac{\rho_{sg}\rho_c}{(\rho_{sg}+\rho_c)}\frac{D}{S}$ and the temperature dependence of the dissipation parameter by formula

$$\beta^2 = 1/\beta_c = \hbar/2eC_J R_N^2 I_C. \tag{4}$$

In our simulations we choose $S = 2.32 * 10^{-10} m^2$ for the area, $T_c = 90K$ for the critical temperature, and $j_c(0) = 9 * 10^6 A/m^2$ at $T = 0$ for the density of critical current. In Ref.[37] the fitting parameters were chosen as $a = 6 * 10^{-4}\Omega m$, $b = 273K$, $c = 24 * 10^{-6}\Omega m/K$, $d = 1.23 * 10^{-2}\Omega m$ as parameter values. Results of simulation are presented in Fig. 3 a. They demonstrate a plateau at small temperatures, maximum at intermediate temperatures and decrease at temperature close to the critical one. An increase in α increases the value of the maximum and shifts it to the smaller temperatures. At small temperature the Zappe curve lies above the $\alpha = 1$ curve, then they coincides practically in some intervals. At high temperature coupling results in high values of return current.

In the second method we used the fitting of the temperature dependence of the dissipation parameter found from the experimentally determined values of C_J, I_c and R_N by formula (4) resulting in $\beta = a + b * \exp(T/c * T_c)$ with $a = 0.01861, b = 5.10414 * 10^{-5}, c = 0.09989$. Result of fitting of the experimental temperature dependence of the critical current by the same formula give us for the same sample $I_c(T) = 1.41667 - 0.39391 * \exp(T/0.79944)$. In Fig. 3 b we present the results of the simulation of the I_r temperature dependence using this fitting formula at three values of coupling parameter: $\alpha = 0.5, 1, 2$. The main features are the same as in previous case, but the Zappe curve shows qualitatively different behavior at low temperatures.

6. Summary and conclusions

Intrinsic Josephson junctions open new ways to realize compact synchronized radiation sources for the THz region. There are many experimental problems which can be solved using results of simulation and modeling. We have reported some results to improve synchronization and the power of radiation by means of adapted shunting. We have also discussed the influence of the return current. Further calculations are necessary for better description of this system to optimize the parameters for applications.

Acknowledgments
This research was partially supported by Heisenberg-Landau Program and the German Research Foundation (DFG). Yu.M.Shukrinov thanks S.Flach and MPIPCS, Dresden, where part of this paper was written.

References

[1] Kleiner R, Steinmeyer F, Kunkel G, Müller P 1992 *Phys. Rev. Lett.* **68** 2394
[2] Kleiner R, Müller, P 1994 *Phys. Rev.* B **49** 1327
[3] Kim S -J, Latyshev Y I, Yamashita T 1999 *Appl. Phys. Lett.* **74** 1156
[4] Yurgens A 2000 *Supercond. Sci. Technol.* **13** R85
[5] Wang H B, Wu P H, Yamashita T 2001 *Phys. Rev. Lett.* **87** 107 002
[6] Wang H B, Wu P H, Yamashita T 2001 *Appl. Phys. Lett.* **78** 4010
[7] Wang H B, Hatano T, Yamashita T, Wu P H, Müller P 2005 *Appl. Phys. Lett.* **86** 023504
[8] Wang HB, Guénon S, Yuan J, Jishi A, Arisawa S, Hatano T, Yamashita T, Koelle D, Kleiner R 2009 *Phys. Rev. Lett.* **102** 017006
[9] Tachiki M, Iizuka M, Minami K, Tejima S, and Nakamura H 2005 *Phys. Rev.* B **71** 34515
[10] Tachiki M, Fukuya S, and Koyama T 2009 *Phys. Rev. Lett.* **102** 127002
[11] Gray K E, Ozyuzer L, Koshelev A E, Kurter C, Kadowaki K, Yamamoto T, Minami H, Yamaguchi M, Tachiki M, Kwok W-K, Welp U 2009 *IEEE Trans. Appl. Supercond.* **19** 886
[12] Saval'ev S, Yampol'skii V A, Rakhmanov A L, Nori F 2010 *Rep. Prog. Phys.* **73** 026501
[13] Hu X, Lin S-Z 2010 *Supercond. Sci. Technol.* **23** 053001
[14] Schmidl F, Pfuch A, Schneidewind H, Heinz E, Dörrer L, Matthes A, Seidel P, Hübner U, Veith M, Steinbeiss E 1995 *Supercond. Sci. Technol.* **8** 740
[15] Haruta M, Kume E and Sakai S 2009 *Supercond. Sci. Technol.* **22** 125004
[16] Seidel P, Schmidl F, Pfuch A, Schneidewind H, Heinz E 1996 *Supercond. Sci. Technol.* **9** A9
[17] Kim S-J, Latyshev YI, Yamashita T 1999 *Appl. Phys. Lett.* **74** 1156
[18] You L X, Torstensson M, Yurgens A, Winkler D, Lin C T, and Liang B 2006 *Appl. Phys. Lett.* **88** 222501
[19] Yurgens A, Torstensson M, You L X, Bauch T, Winkler D, Kakeya I, Kadowaki K 2008 *Physica C* **468** 674
[20] Koval Y, Jin X, Bergmann C, Simsek Y, Ozyuzer L, Müller P, Wang H, Behr G, Büchner B 2010 *Appl. Phys. Lett.* **96** 082507
[21] Chana O S, Kuzhakhmetov A R, Warburton P A, Hyland D M C, Dew-Hughes D, Grovenor C R M 2000 *Appl. Phys. Lett.* **76**, 3603
[22] Mans M, Schneidewind H, Buenfeld M, Schmidl F, Seidel P 2006 *Phys. Rev.* B **74** 214514
[23] Grib A N, Mans M, Scherbel J, Buenfeld M, Schmidl F, Seidel P 2006 *Supercond. Sci. Technol.* **19** S 200
[24] Grib A N, Seidel P, Scherbel J 2002 *Phys. Rev.* B. **65** 94508
[25] Seidel P, Grib A N, Shukrinov Yu M, Scherbel J, Hübner U, Schmidl F 2001 *Physica* C **362** 102
[26] Wang H B, Aruga Y, Chen J, Nakajima K, Yamashita T, Wu P H 2000 *Appl. Phys. Lett.* **77** 1017
[27] Tachiki M, Iizuka M, Minami K, Tejima S, and Nakamura H 2005 *Phys. Rev.* B **71** 134515
[28] Grib A, Seidel P 2009 *Physica Status Solidi RRL* **3** 302
[29] Machida M, Koyama T, Tanaka A and Tachiki M 2000 *Physica* C **85** 330
[30] Shukrinov Yu M, Mahfouzi F, Seidel P 2006 *Physica* C **62** 449
[31] Shukrinov Yu M, Mahfouzi F 2007 *Phys.Rev.Lett.* **98** 157001
[32] Shukrinov Yu M, Mahfouzi F, Pedersen N F 2007 *Phys. Rev.* B **75** 104508
[33] Zappe HH 1973 *J. Appl. Phys.* **44** 1371
[34] Heine G, Lang W, Wang X L, and Dou S X 1999 *Phys. Rev.* B **59** 11179
[35] Ambegaokar V and Baratoff A 1963 *Phys. Rev. Lett.* **10** 486
[36] Yurgens A, Winkler D, Zavaritsky N V, and Claeson T 1997 *Phys. Rev. Lett.* **79** 5122
[37] Okanoue K and Hamasaki K 2005 *Appl. Phys. Lett.* **87** 252506